Available online at www.sciencedirect.com
ScienceDirect
Journal of Photochemistry and Photobiology A: Chemistry 187 (2007) 45–52
Journal of Photochemistry and Photobiology A:Chemistry
www.elsevier.com/locate/jphotochem

Characterization of methylene blue/TiO_2 hybrid thin films prepared by the liquid phase deposition (LPD) method: Application for fabrication of light-activated colorimetric oxygen indicators

David Gutiérrez-Tauste [a,*], Xavier Domènech [a], Nieves Casañ-Pastor [b], José A. Ayllón [a]

[a] *Chemistry Department, Autonomous University of Barcelona, Campus UAB, Building Cn, 08290 Cerdanyola del Vallès, Barcelona, Spain*
[b] *Institute of Materials Science (CSIC), Campus UAB, 08290 Cerdanyola del Vallès, Barcelona, Spain*

Received 6 July 2006; received in revised form 20 September 2006; accepted 21 September 2006
Available online 30 September 2006

Abstract

Methylene blue (MB)/TiO_2 hybrid nanocomposite material has been successfully deposited on both bare glass and indium tin oxide (ITO) covered glass by the liquid phase deposition (LPD) technique. LPD method is applied to one-step hybrid dye/TiO_2 deposition. An optimized amount of MB is added to the fluoride titania precursor aqueous solution in order to entrap this dye within the growing thin film of TiO_2, yielding a MB/TiO_2 nanocomposite material. Stable, well-adhered, intense blue-colored and optically transparent coatings have been obtained. The formation of the material can be explained by electrostatic interaction between negative charge density at the fluorinated surface of TiO_2 and the cationic dye. MB/TiO_2 nanocomposite material has been characterized by ATR-FT-IR, UV–vis spectroscopy, SEM, TEM, grazing angle XRD and cyclic voltammetry (CV). Deposited hybrid films exhibit photochemical activity: MB is photobleached upon UVA irradiation, using triethanolamine (TEOA) as mild sacrificial electron donor. Moreover, light-activated oxygen indicators with high optical transparency and delayed response can also be satisfactory fabricated by spin-coating a solution of TEOA with an encapsulating polymer (hydroxyethyl cellulose) over the MB/TiO_2 hybrid films.

Keywords: Titanium oxide; Methylene blue; Liquid phase deposition; Hybrid nanocomposite; Light-activated oxygen indicator

1. Introduction

Liquid phase deposition (LPD) is a soft chemical technique first described in the patent literature to deposit titania films [1] and have been successfully applied to the deposition of many oxides. LPD of titania thin films has been studied throroughly by several groups [2–12]. Titanium dioxide (TiO_2) thin films deposited by this method are of interest for diverse applications including deposition of inorganic micropattern on flexible substrates [4], inorganic barrier layer to physically block oxidation of polymeric materials [7], photocatalyst-supported materials [11,12], blocking layer on dye sensitized solar cells [13], or superhydrophilic self-cleaning surfaces [14].

LPD is a process based on the controlled hydrolysis of metallic fluoro-complexes. The dynamic equilibrium exchange established between fluoro and water ligands is displaced towards TiO_2 formation in the presence of a fluoride scavenger such as boric acid. Partially crystallized TiO_2 deposition can be obtained by LPD at relatively low temperature (below 80 °C) [15,16]. Anatase formation is favored in presence of titanium complexing ions such as fluoride, being this phase usually produced by LPD [17]. This wet process allows to deposit TiO_2 over large and complex surfaces without thermal annealing. The key reactions can be expressed as follows:

$$TiF_6^{2-}(aq) + 2H_2O \rightleftarrows TiO_2(s) + 4\,HF(aq) + 2F^-(aq)$$

$$H_3BO_3(aq) + 4HF(aq) \rightarrow BF_4^-(aq) + 3H_2O(l) + H^+(aq)$$

Surface modification of TiO_2 semiconductor particles has gained much attention due to the application of these materials in fields as diverse as electrochromic [17] and photochromic [18] devices, dye-sensitized solar cells [19] and light-induced site-specific DNA redox chemistry [20]. In these applications, transparent conductive materials must be used as substrates for

* Corresponding author. Tel.: +34 93 5812176; fax: +34 93 5812920.
E-mail address: davidg@qf.uab.es (D. Gutiérrez-Tauste).

1010-6030/$ – see front matter © 2006 Published by Elsevier B.V.
doi:10.1016/j.jphotochem.2006.09.011

modified TiO_2 particles films. More than one step is usually required to produce these complex nanostructures: the linking of semiconductor particles to form a more or less porous film and, ideally, the adsorption of a monolayer of the surface modifier. When typical TiO_2 deposition processes as sol–gel or doctor blade are used, post-annealing treatments at 400–500 °C are required to sinterize TiO_2 particles or to induce crystallization [17,21]. Thus, thermolabile substrates cannot be used. On the other hand, the surface modification process is a time consuming step, as TiO_2 films must be put in contact with surface modifier solution for a long period to allow diffusion and equilibration into the intricate porous structure. Development of simpler, low temperature and one-step methods is attractive to advance in the application of hybrid organic-TiO_2 films.

One-step deposition methods for hybrid TiO_2 films are poorly reported in the literature. Electrochromic electrodes were prepared by electrochemical deposition of Prussian Blue in the presence of a suspension of TiO_2 particles [22]. Rhodamine-doped SiO_2/TiO_2 composite films were fabricated by the sol–gel technique with low temperature heat treatment at 150 °C [23]. Organic dyes were entrapped within TiO_2 thin films prepared on conductive substrates by electrodeposition from classical sol–gel titania precursors [24]. Stucky et al. have reported a new fluorocarbon-based synthesis route for hybrid rhodamine/TiO_2 mesostructured optical materials for waveguided photoluminescence emission device [25]. Recently, Deki et al. have reported the deposition of alkyl sulfate and alkylbenzene sulfonate surfactants/TiO_2 [26] and copper phthalocyanine/TiO_2 [27] hybrid films by the LPD method. Hu et al. have reported moleculary imprinted TiO_2 thin films by LPD for the determination of L-glutamic acid [28]. However, one-step hybrid film deposition has been described for other transition oxides such as ZnO [29,30] and SiO_2 [31,32].

Methylene blue (MB) is a cationic dye whose redox formal potential, comprised between 0.08 and −0.25 V (versus SCE) in solution with pH 2–8, respectively, is close to those of several biomolecules [33]. MB has been widely used for electrochemical applications, for example, as catalyst/mediator in electrochemical biosensors [33]. Moreover, TiO_2 has been satisfactory sensitized with MB for photodegradation of various halocarbons using visible light [34]. Recently, a mixture of commercial TiO_2 powder and MB has been used to fabricate an intelligent ink sensible to oxygen [35,36]. Oxygen allows to grow aerobic microorganism during food storage, being the main cause of most food-spoilage. There is an increasing interest to develop inexpensive, non-toxic and irreversible oxygen sensors in fields as modified atmosphere food (MAP) packaging to assure oxygen absence [35,36].

Here, we report, for the first time, an one-step route to entrap MB with TiO_2 chemically deposited in situ by the LPD technique. MB/TiO_2 resulting films consist of anatase nanocrystals with adsorbed MB molecules. MB/TiO_2 nanocomposite hybrid films were characterized by ATR-FT-IR, UV–vis spectroscopy, SEM, TEM, grazing angle XRD and cyclic voltammetry (CV). Photochemical activity of the films were tested and light-activated oxygen indicators were satisfactory fabricated from the deposited nanocomposite material.

2. Experimental section

2.1. Reagents

Ammonium hexafluorotitanate, boric acid, methylene blue (MB) and hexafluorotitanic acid were analytical grade (Aldrich, Panreac) and used as received without further purification. Acetone and ethanol (Panreac) were used for substrate cleaning. TiO_2 Degussa P-25 (80% anatase–20% rutile) was kindly provided by Degussa (Spanish branch). Deionized water from a Milli-Q system (Millipore, conductivity <0.05 μS/cm) was used both in solution preparation and cleaning procedures.

2.2. Substrates

The substrates used were ITO (In_2O_3:Sn) conducting glass, 13–18 Ω/sq, 1.1 mm thick (Optical Filters) and bare glass (microscope slides, IDL). Substrates were cleaned just before performing the deposition process [15]. Glass slides were sequentially immersed for 15 min in boiling 50% sulfuric acid and 15 min in boiling water, followed by 5 min ultrasonic cleaning in acetone, then absolute ethanol and finally water. ITO-glass substrates were subjected to 5 min ultrasonic cleaning in acetone, then in absolute ethanol, then in 30% nitric acid for 1 min and finally in water 5 more min.

2.3. Deposition of TiO_2 films

TiO_2 films were deposited on both, glass slides and ITO-covered glass, according to LPD procedure described in our previous work [15]. These samples were used for comparative purposes. Bare glass substrates were pretreated in a 0.10 mM H_2TiF_6 solution, with pH adjusted to 3.2 using diluted NH_3, at 80 °C for 30 min. After this pretreatment, the substrate was sonicated in water and used immediately. Substrates were placed vertically into a polyethylene vessel containing the fresh precursor solution (10 mM $(NH_4)_2TiF_6$ and 30 mM H_3BO_3, pH adjusted to 2.8 using diluted $HClO_4$). The whole was sonicated for 1 min and kept at 80 °C for 3 h. After deposition, films were gently washed with water and dried with a nitrogen gas flow.

2.4. Deposition of MB/TiO_2 films

In this case, both substrates had to be pretreatred. Bare glass slides were pretreated as in the former case. ITO-glass substrates were pretreated for 1 h at 80 °C in an aqueous solution 10 mM $(NH_4)_2TiF_6$ and 30 mM H_3BO_3 at natural pH of 3.6. In both cases, substrates were sonicated after the pretreatment and the subsequent deposition process were also performed immediately. The optimized precursor bath consisted of 10 mM $(NH_4)_2TiF_6$, 30 mM H_3BO_3 and 0.5 mM MB; its initial pH was adjusted to 2.8 with diluted $HClO_4$. A range of MB concentrations between 0.1 mM and 2 mM were also tried. The substrates were immersed in the bath, sonicated for 1 min, and kept at 80 °C for 4.5 h. After LPD process, samples were also gently washed with water and dried with a nitrogen gas flow.

2.5. Characterization

ATR-FT-IR spectrums were performed with a Bruker apparatus (Tensor model equipped with MKII Golden Gate). TiO_2 powder samples from the films were obtained by scrapping the coating off. UV–vis absorbance data were obtained with a Heλios series γ spectrophotometer (Bonsai Technologies), using the respective bare substrate as the blank. Films surface characteristics were investigated by SEM on gold covered samples, using a Hitachi S-570 microscope (operating voltage, 10–30 kV). For thickness measurements, samples were cut into pieces which results in breaking the TiO_2 film near the cut edge of the substrate. Films thickness was studied in these edges, taking into consideration the sample inclination with respect to the electron beam. Electron diffraction patterns and transmission electron microscopy (TEM) images were recorded in a JEOL 2011 microscope that was operated at 200 kV. Energy dispersive spectroscopy (EDS) X-ray microanalysis were carried out using an INCA-X detector (Oxford Instruments). XRD spectra were registered on a Philips X'Pert diffractometer equipped with a monochromator and using Cu Kα radiation (λ = 0.154056 nm). In order to increase the sensitivity of the thin film signal, a grazing incident configuration was used (2.0°). Cyclic voltammetry (CV) studies were carried out on an EG&G PAR 273A potentiostat/galvanostat at room temperature. A three-electrode electrochemical cell were used on a single compartment: MB/TiO_2 films deposited on ITO-covered glass were used as working electrode (a Cu foil-Sn clad conductive tape with an Ag adhesive (BDF Tesa) was employed to assure good electrical contact on ITO), a platinum wire (1 mm diameter) served as counter electrode and a Ag/AgCl double bridged (1 M KCl) electrode was used as the reference. The electrolyte was a 0.25 M aqueous solution of tetrabutylammonium chloride (TBACl) with pH adjusted to 2.5 with diluted hydrochloric acid. Cathodic run and anodic run were performed at scan rate of 5 and 10 mV/s, respectively. Argon was flowed through the electrolyte solution just before performing the CV.

To test the adhesion and stability of the MB/TiO_2 films ultrasound disruption was used: coated substrates were immersed completely in a beaker with water and sonicated for 5 min (Ultrasonic bath Selecta, 50 W). For comparison purposes, MB were adsorbed on TiO_2 Degussa P-25 from a suspension 10 mM TiO_2 P-25 and 0.5 mM MB. The initial pH was adjusted to 2.8 with diluted $HClO_4$ and the suspension was kept at 80 °C for 4.5 h. The powder obtained was separated by centrifugation, washed with deionized water and dried at 60 °C.

UV-activated colorimetric oxygen indicators devices were fabricated using MB/TiO_2 films deposited on glass. An upper layer of triethanolamine (TEOA) embedded in hydroxyethyl cellulose (HEC) polymer were spin-coated at 1000 rpm for 5 min, using an aqueous solution of 7.5 g TEOA and 2.5 g HEC in 50 ml of water. Photobleaching experiments were carried out upon exposure of UVA light from a 6 W Phillips black light (held 2.5 cm away) on both MB/TiO_2 oxygen sensors and MB/TiO_2 bare coatings (immersed in a 0.1 M TEOA aqueous solution). Lamp intensity at the coatings was 1.4 mW/cm^2, measured using a UV radiometer Lutron UVA-365. Samples photobleaching were followed by UV–vis absorbance spectra in the 400–800 range.

3. Results and discussion

3.1. MB/TiO_2 films preparation and characterization

Our first goal was to find bath compositions and substrate preparation procedures that allow to obtain optically transparent and well adhered coatings of a MB/TiO_2 nanocomposite material, that is TiO_2 nanocrystals grown on the substrate with MB modifier adsorbed on their surface. For that purpose, several assays varying MB concentrations in the LPD precursor bath were carried out.

It is important to remark that high coating thickness covering the substrate or excessive MB incorporation within the TiO_2 growing film impede the deposition of well adhered coatings. In addition, to guarantee its further use in several applications it is desirable that all TiO_2 nanoparticles are directly connected between them. On the other hand, at very low MB concentration, its incorporation into the coating is very poor and thus practically almost pure TiO_2 film is obtained. Using an optimized 0.5 mM MB concentration in the precursor bath, uniform intense blue-colored films were obtained without TiO_2 homogeneous precipitation. Films adhesion and MB desorption were tested using ultrasound disruption.

In fact, the actual MB concentration in solution is slightly lower than the nominal one due to the formation of a flocculent violet precipitate corresponding to the perchlorate salt of MB cation that is less soluble that the chloride salt used as starting. This precipitate was observed in the LPD precursor bath just after adjusting initial pH to 2.8 with diluted perchloric acid. $MBClO_4$ was also identified by IR spectroscophy (Fig. 1d) [37]. Although the formation of this precipitate can be prevented by using a different acid to adjust the pH of the bath, experimental

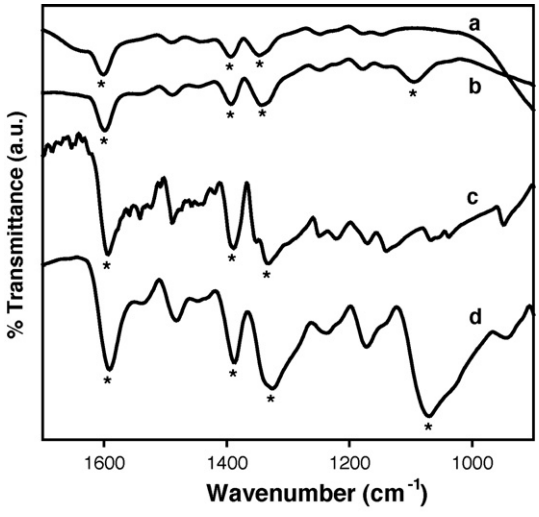

Fig. 1. ATR-FT-IR spectra of: (a) MB/TiO_2 film scrapped off, (b) MB adsorbed on Degussa P-25, (c) commercial MB, and (d) $MBClO_4$ precipitate from the LPD solution after MB/TiO_2 film deposition. Mean absorption peaks are also marked with '*'.

results show that this precipitate, that remain at the bottom of the container does not interfere with the formation of an uniform coating. A set of additional experiments were performed avoiding the precipitation of the perchlorate salt of MB, using dye concentrations near the reported solubility value for $MBClO_4$ ($1–3 \times 10^{-5}$ M) [44] and adjusting the pH of the bath to 2.8 with HCl. In these experiments, no satisfactory hybrid film deposition was observed, suggesting that precipitated $MBClO_4$ allow to preserve a MB concentration during the LPD process. Moreover, the existence of an optimal MB concentration suggest that $MBClO_4$ redisolution when MB soluble is incorporated within the TiO_2 film can be limited kinetically.

TiO_2 prepared by LPD process present a high degree of surface fluorination (≡Ti–F) [10,15]. The fluoride chemisorption is favored at acidic pH (maximum of approximately 99% at pH 3–4) and greatly reduces the positive surface charge on TiO_2 by replacing $\equiv Ti–OH_2^+$ by ≡Ti–F species [38]. Due to the great affinity of fluoride for the TiO_2 surface, MB direct adsorption on the oxide surface is avoided in a high fluorinated surface.

Characteristic infrared absorption peaks of MB [33,39] (Fig. 1c) at ∼1600 cm^{-1} (ring stretch), ∼1390 cm^{-1} (C–N symmetric stretch) and ∼1335 cm^{-1} (–CH_3 symmetric deformation) appear in the MB/TiO_2 nanocomposite material (Fig. 1a). MB/TiO_2 and MB adsorbed on Degussa P-25 present almost the same IR spectra (Fig. 1a and b, respectively). The only difference is the peak at ∼1087 cm^{-1} of P-25/MB powder, associated to stretching vibrations of perchlorate anion [37] and is not observed in the MB/TiO_2 fluorinated material. These results point to a similar adsorption mode for the cationic dye on both a clean and a fluorinated surface. It is thought therefore, that the electrostatic interaction between negative density charge at the TiO_2 fluorinated surface generated during the LPD process and the cationic dye ($(\equiv Ti\text{-}F^{\delta-}:::MB^+)$) will be the force responsible of MB adsorption, yielding the final MB/TiO_2 nanocomposite material.

The intense coloration of the MB/TiO_2 hybrid films deposited suggest that the nanocomposite contains dye molecules in a high concentration. MB adsorbed on clean (non-fluorinated) TiO_2 surface desorbs quickly in an aqueous medium. However, MB of MB/TiO_2 films only desorbs appreciably after approximately 10 days of immersion in water, even if an electrolyte salt is added to the medium, i.e. KCl, NaCl, NH_4Cl or $Na(OOC–H_3C)$. A reference experiment trying to incorporate MB from an aqueous solution to a TiO_2 blank film also obtained by LPD over one night showed very low MB adsorption.

UV–vis optical absorption of a typical MB/TiO_2 film presents a non-symmetrical peak with a maximum at 580 nm and a shoulder at approximately 700 nm (Fig. 2). The shift towards shorter wavelength, with respect to the MB monomer ($\lambda_{max} = 664$ nm), clearly denotes that MB cations are aggregated. The position of the maximum and the shape of the signal suggest that MB is mainly present as trimers, while the presence of monomers is significantly low [40–43]. Performance studies of oxygen indicators fabricated using MB/TiO_2 films confirm that MB cations are aggregated (see discussion of Fig. 6 in Section 3.2). On the other hand, UV–vis spectrum of the deposition bath shows mainly presence of monomer, according to the $MBClO_4$ solubility in water reported [44] ($1–3 \times 10^{-5}$ M) and taking into account that formation of MB aggregates is reported for [MB] $>10^{-4}$ to 10^{-3} M [41]. Self-aggregation is then favored by adsorption and concentration within the film. The aggregation of MB and the consequent hypsochromic shift of the visible spectra has been reported when cationic dyes are adsorbed on negatively charged surfaces [45,46]. In the MB/TiO_2 nanocomposite material, the TiO_2 nanocrystals can wear a neat negative charge due to excess fluoride adsorbed on the titania surface that counteract the positive charge of the MB cations. Thus, most probably, the dye is adsorbed on the fluoride layer and not directly on the oxide surface. The base line of MB/TiO_2 spectrum shows a slight decrease of transmittance with respect the case of TiO_2 (compare in the 400–450 nm interval), due to some degree of light dispersion as consequence of the film morphology.

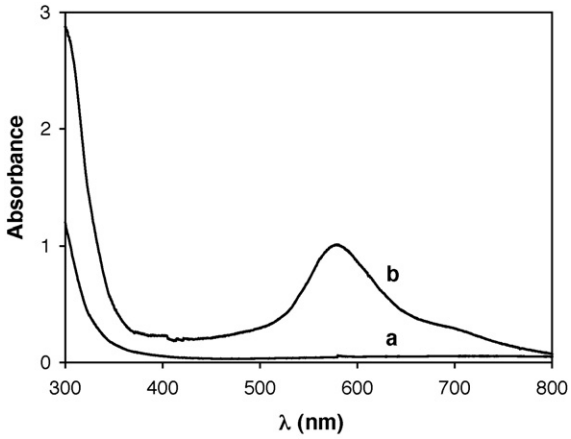

Fig. 2. Typical UV–vis absorption spectra of films deposited on glass slides by LPD: (a) TiO2 and (b) MB/TiO_2.

Surface morphology and thickness of MB/TiO_2 hybrid films deposited on glass slides were studied by SEM (Fig. 3a and b). MB/TiO_2 films show dense and compact substrate coverage, nevertheless their film surface are slightly waved. However, MB/TiO_2 samples show no cracks and present high optical transparency (see Fig. 2, absorbance UV–vis). The particle size in the MB/TiO_2 samples is in the 15–50 nm range, being clearly lower with respect to TiO_2 samples [15]. An average deposition rate of 105 nm/h is estimated taking into account the films thickness (Fig. 3b) and the deposition time in MB/TiO_2 samples. For comparison, a deposition rate of 85 nm/h was reported for TiO_2 films in our previous work [15]. SEM observations point that MB adsorption on the fluorinated TiO_2 surface limit the particle size of the new material and also increase slightly the average deposition rate of the film.

To improve our understanding of the MB/TiO_2 hybrid nanocomposite material, TEM and selected-area electron diffraction (SAED) studies were carried out (Supporting Information). The film studied was deposited using a 1 mM MB concentration in the deposition bath in order to obtain a coating with less adherence. Film was sonicated for 15 min in ethanol to detach nanocomposite aggregates of appropriate size to be observed by TEM. The diffraction pattern indicates a polycrystalline structure with diffraction rings corresponding to lattice

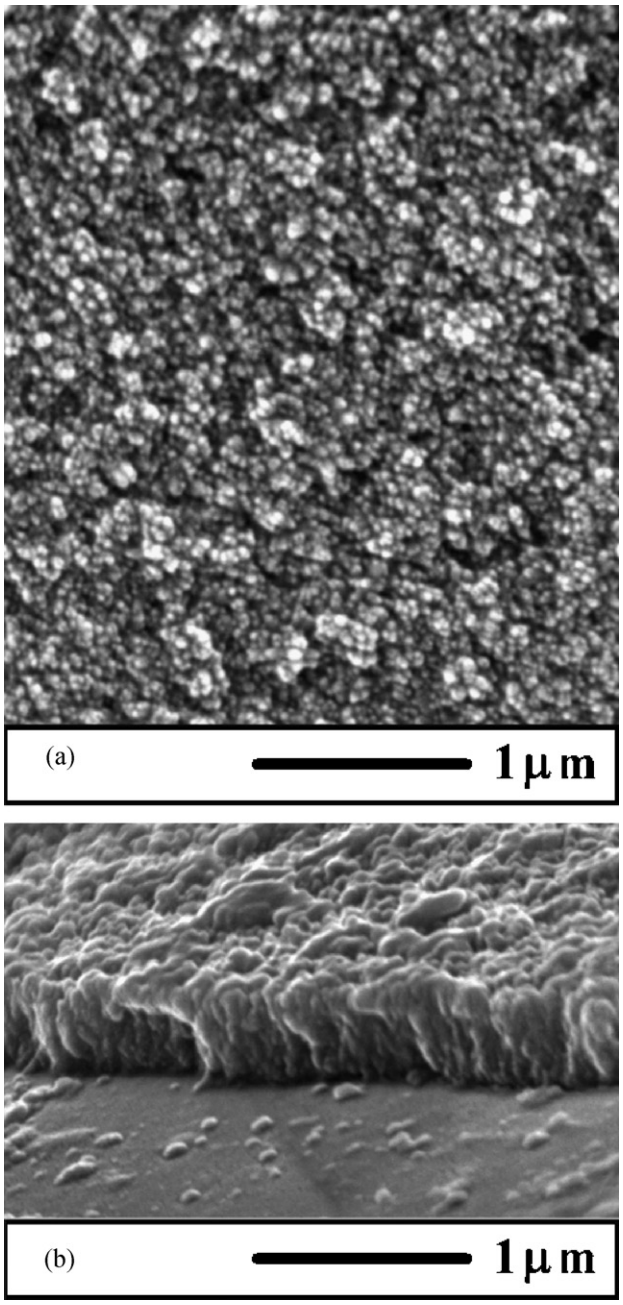

Fig. 3. SEM photographs showing surface morphology (a) and film thickness (b) of MB/TiO_2 samples deposited on glass by LPD.

spacings of 3.5 and 2.4 Å that are assigned to (1 0 1) and (0 0 4) reflections of anatase TiO_2 (JCPDS pattern 21–1272). These lattice fringes of the anatase grains are easily distinguished in the corresponding TEM image. The associated EDS microanalysis (Supporting Information) show a sulfur atomic percentage of approximately 2%. Taking into account that every MB molecule only have one sulfur atom, microanalysis results point the incorporation of the dye at high concentration within the film.

X-ray diffraction of TiO_2 and MB/TiO_2 films deposited on glass slides are shown in Fig. 4, revealing peaks that may be assigned to the anatase structure. It is well known that anatase is the TiO_2 phase usually favored by LPD, due to the presence of

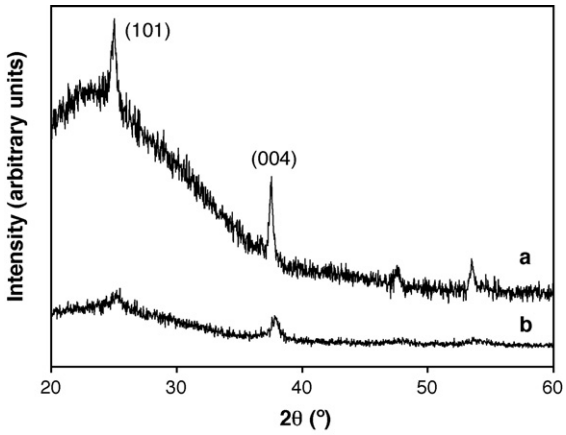

Fig. 4. Grazing-incidence XRD diffractogram of films deposited on glass slides by LPD: (a) TiO_2 and (b) MB/TiO_2.

titanium strongly complexing ions such as the fluoride [6,15,16]. Relative intensities of the peaks differ noticeable respect to the anatase standard (JCPDS pattern 21–1272), corresponding to complete random order. Thus, the standard presents a relative intensity of 5:1 for the (1 0 1) and the (0 0 4) peaks. However, in the diffractrograms obtained, the relative intensity of the (0 0 4) signal appears notably increased. Preferential *c* axis orientation has been reported previously both for TiO_2 films and powders prepared by LPD, and has been attributed to the preferential adsorption of fluoride to planes parallel to this direction [7,8]. On the other hand, although MB/TiO_2 films are thicker than TiO_2 ones, their diffraction signals are weaker and wider. In addition, while MB/TiO_2 films present approximately a 2:1 relative intensity for (0 0 4) and (1 0 1) signals, the TiO_2 samples only present a 1:1 ratio. XRD results confirm that MB adsorption on fluorinated surface of the new material is favored, limiting the size of anatase crystallites (and also decreasing the main particle size as was observed by SEM) and yielding more oriented films.

3.2. Photochemical activity: light-activated oxygen indicators

A set of preliminary experiments were performed to evaluate the photochemical activity of the new material. MB/TiO_2 films were immersed in a TEOA solution and were UV-irradiated. In these experiments, electron–hole pairs are generated in the semiconductor particles. Photogenerated holes are able to oxidize irreversibly the TEOA mild sacrificial electron donor while photogenerated electrons reduce the MB dye to its leuco form. Upon irradiation with UVA light, under aerobic or anaerobic conditions, initial highly blue-colored samples were completely bleached showing excellent transparency. Samples remain indefinitely bleached in the absence of oxygen, whereas blue color begin to return as soon as ambient oxygen reoxidize leuco-MB. Maximum coloration recovery is attained after approximately 1 h under ambient conditions. It is important to remark that MB desorption in the TEOA solution is not observed in any case.

UV-activated colorimetric oxygen indicators devices were satisfactory fabricated from MB/TiO_2 films, by spin-coating a TEOA solution containing HEC as encapsulating polymer over

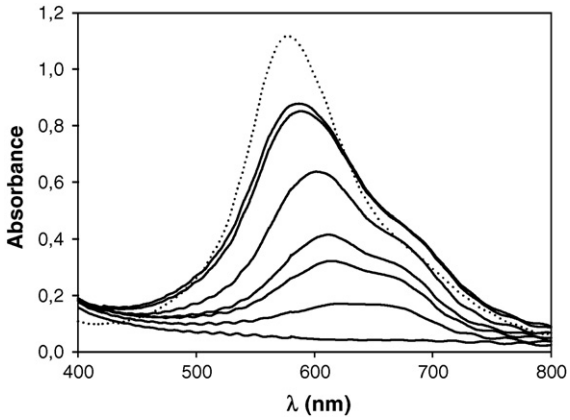

Fig. 5. Absorbance changes in a typical MB/TiO_2 UV-activated oxygen indicator between 400 and 800 nm, after different times under ambient conditions (solid line from bottom to top): 0, 4, 8, 12, 24, 48 and 72 h, respectively. Initial spectra of the non-activated TiO_2/MB oxygen indicator is also included (dotted line).

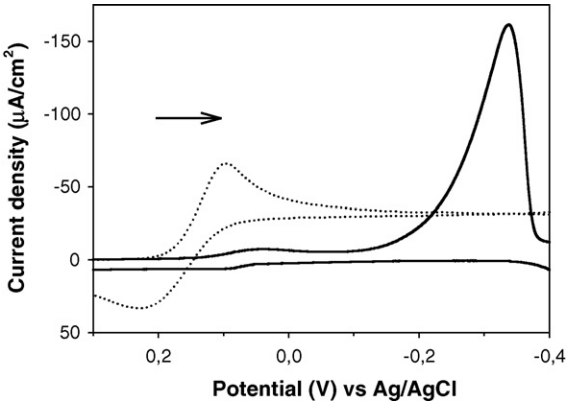

Fig. 6. Typical CV of MB/TiO_2 films deposited on ITO-coated glass (solid line) and CV of the blank experiment with MB in solution (dotted line). Electrolyte: 0.25 M TBACl; cathodic scan rate: 5 mV/s; anodic scan rate: 10 mV/s.

the nanocomposite material in an analogous way to intelligent inks previously reported by Mills et al. [35,36] MB/TiO_2 oxygen indicators are UV-activated (totally bleached state) in an irradiation time of 18 to 48 h. The low photocatalytic activity of the TiO_2 deposited due to its low crystallinity seems to increase the irradiation time required to activate the indicator. A decrease in activation time is expected using UVA lamps with higher power.

Leuco-MB reoxidation under ambient atmospheric conditions was studied following evolution of the UV–vis spectra (Fig. 5, solid lines). Displacement of the maximum of the peak to shorter wavelengths as reoxidation advance denotes reaggregation of MB. MB/TiO_2 sensors show a delayed response to oxygen presence, pointing a slow oxygen diffusion through the indicator. A delayed response of the indicator could be useful to estimate the exposition time to air [36]. Maximum absorbance recovery at 580 nm is typically 75–80% with respect to the initial absorbance (Fig. 5, dotted line). However, spectra corresponding to a reoxidized sample after 48 or 72 h under ambient conditions present higher MB monomer absorbance at 664 nm than the original spectra, indicating a higher amount of monomer. Therefore, the change in absorbance spectra is due to a different distribution of aggregates rather than to partial decomposition. It must be considered that molecular diffusion of MB may be prevented or made more difficult because of the solid nature of the MB/TiO_2 nanocomposite. Minor MB direct photolysis can also partially account for the spectra variations [47]. Therefore, although MB/TiO_2 oxygen indicators can be reused there are minor variations after each cycle, pointing a limited stability of the device.

3.3. Cyclic voltammetry experiments

MB/TiO_2 films were also satisfactory prepared on a conductive substrate, i.e. ITO-covered glass. While regular and dense TiO_2 coatings were deposited on ITO without any pretreatment [14], only hazy and low-colored MB/TiO_2 samples could be obtained on ITO substrate. Pretreatment of the surface is absolutely necessary to prepare MB/TiO_2 coatings on ITO; MB adsorption on ITO seems to make difficult the nucleation of TiO_2 particles. Thus, a preliminary seed process is required to assure enough TiO_2 nucleation sites density before the deposition process. Otherwise, only a partial substrate coverage can be attained and low-transparency samples are obtained. Modification of the substrate upon treatment is too slight to be clearly measured or identified by the characterization techniques used in this work.

Cyclic voltammetry (CV) experiments of MB/TiO_2 films deposited on ITO-covered glass (Fig. 6, solid line) show redox activity, evidencing the electroactive properties of the nanocomposite material. Two cathodic waves that shift their potential value upon repeated cycling are observed, showing the irreversibility of the electrochemistry of the MB/TiO_2 nanocomposite material in the CV time scale. A couple of cathodic/anodic peaks of marginal current density is seen with a midpoint potential of approximately +70 mV. A CV blank experiment of dissolved MB using ITO as electrode (Fig. 6, dotted line) show a cathodic/anodic couple with a midpoint potential of +163 mV. Taking into account that only MB monomers are expected in the TBAC1 solution [48], the couple has to be assigned to MB redox activity in the monomer form. In addition, Garrone et al. observed a similar couple in CV of MB solutions using a paste graphite electrode and ascribed it to traces of MB in the salt form, strongly interacting with its chloride counted on physisorbed on carbon grains [49]. Therefore, the marginal couple in the MB/TiO_2 nanocomposite have to be ascribed to MB traces in the salt form on the ITO surface. However, the marginal anodic peak in the nanocomposite is preferably observed at higher scan rates (10 mV/s) than the cathodic one (5 mV/s), suggesting that reoxidation of traces of this MB salt form is a faster process.

A second cathodic wave of high current density at −338 mV versus Ag/AgCl is seen in the MB/TiO_2 material (Fig. 6, solid line). This cathodic signal is assigned to MB reduction in the MB/TiO_2 nanocomposite and, consequently, total bleaching of the film is observed. The MB reduction potential is noticeably increased in the nanocomposite with respect to the MB reduction of the monomer form in solution seen in the blank experiment ($E_{cathodic}$ = +96 mV, dotted line in Fig. 6). Different facts can contribute to difficult the MB reduction in the nanocomposite:

MB self-aggregation, MB electrostatic interaction on the fluorinated TiO_2 surface or the low conductivity of the TiO_2 due to its semiconductor nature. The main reduction peak in the MB/TiO_2 nanocomposite presents a non-symmetrical appearance, also suggesting irreversibility of the MB reduction process in the time scale studied. The anodic couple of this main MB cathodic peak is not present in the 0.5–10 mV/s scan rate range studied, pointing the leuco-MB reoxidation cannot be accelerated electrochemically. While after the cathodic run total bleaching of the MB/TiO_2 electrode is observed due to reduction of the greater part of the MB molecules, after the anodic run only a slight blue coloration can be distinguished in the electrode that can be assigned to the secondary oxidation process of the MB salt form. However, under atmospheric conditions blue coloration returned to the film after the CV experiment and self-aggregation of MB is also observed by UV–vis spectroscopy.

It has also been observed that electrolytic reduction of MB induces its desorption from the coating, with clear evidence of electrolyte-blue coloring after oxidation. MB desorption values of $1.5–4 \times 10^{-9}$ mol/cm^2 are estimated by UV–vis spectroscopy in the electrolyte solution considering that only MB monomers are present ($\varepsilon_{664} = 9 \times 10^{-4}\ M^{-1}\ cm^{-1}$) [41]. Air was flowed through the electrolyte solution to assure leuco-MB reoxidation to MB form. No MB readsorption is observed in CV experiments time scale. Therefore, the absence of the main MB anodic peak could be attributed to a very slow electrochemical oxidation kinetics and changes in the interaction among the electroactive MB molecules and the fluorinated TiO_2 surface, that favor the MB desorption after the cathodic run. It must be remembered that no MB desorption was observed in photobleaching experiments using TEOA as sacrificial electron donor (see Section 3.2, *Photochemical activity*). MB/TiO_2 nanocomposite seems to follow different redox mechanisms in CV electrochemical processes with respect to photochemical reduction and chemical oxidation by atmospheric oxygen.

4. Conclusions

MB/TiO_2 nanocomposite thin films have been successfully prepared by LPD on both bare glass and ITO-covered glass, concluding that new applications of LPD method are possible in the field of the preparation of organic-inorganic hybrid thin films. High concentrations of MB are incorporated in the new nanocomposite material, yielding stable, well-adhered, intense blue-colored and optically transparent coatings. MB adsorption on the fluorinated TiO_2 surface promotes MB aggregation, limits the size of anatase crystallites and the main particle of the nanocomposite, while slightly increases the average deposition rate of the film. The results seem to be reasonably explained by continuous electrostatic interaction among negative density charges at the fluorinated surface and the cationic dye molecules during the LPD process. The MB/TiO_2 films exhibit photochemical activity respect to the oxidation of TEOA mild sacrificial electron donor upon UVA irradiation. Light-activated oxygen indicators with high optical transparency and delayed response can also be satisfactory fabricated from the MB/TiO_2 hybrid films. CV experiments show irreversible redox activity of the MB/TiO_2 nanocomposite in the time scale studied and provide indications that different mechanisms can take place in CV electrochemical processes (MB desorption) with respect to photochemical reduction and chemical oxidation by atmospheric oxygen (non MB desorption).

Acknowledgements

This work has been financed by the Spanish National Plan of Research (BQU2003-01280 project). We thank Jose Manuel Amigo for useful discussion about the UV–vis spectra.

Appendix A. Supplementary data

Supplementary data associated with this article can be found, in the online version, at doi:10.1016/j.jphotochem.2006.09.011.

References

[1] H. Kawahara, H. Honda, Japanese Patent 59141441 A (Nippon Sheet Glass), August 14, 1984.
[2] S. Deki, Y. Aoi, O. Hirió, A. Kajinami, Chem. Lett. 6 (1996) 433–434.
[3] H.Y.Y. Ko, M. Mizuhata, A. Kajinami, S. Deki, J. Flu. Chem. 120 (2003) 157–163.
[4] A. Dutschke, D. Diegelmann, P. Löbmann, J. Mater. Chem. 13 (2003) 1058–1063.
[5] Y. Masuda, T. Sugiyama, W.S. Seo, K. Koumoto, Chem. Mater. 15 (2003) 2469–2476.
[6] H. Pizem, C.N. Sukenik, U. Sampathkumaran, A.K. McIlwain, M.R. De Guire, Chem. Mater. 14 (2002) 2476–2485.
[7] H. Pizem, O. Gershevitz, Y. Goffer, A.A. Frimer, C.N. Sukenik, U. Sampathkumaran, X. Milhet, A. McIlwain, M.R. De Guire, M.A.B. Meador, J.K. Sutter, Chem. Mater. 17 (2005) 3205–3213.
[8] A.M. Peiró, E. Vigil, J. Peral, C. Domingo, X. Domènech, J.A. Ayllón, Thin Solid Films 411 (2002) 185–191.
[9] J.A. Ayllón, A.M. Peiró, L. Saadoun, E. Vigil, X. Domènech, J. Peral, J. Mater. Chem. 11 (2000) 1911–1914.
[10] J.G. Yu, H.G. Yu, B. Cheng, X.J. Zhao, J.C. Yu, W.K. Ho, J. Phys. Chem. B 107 (2004) 13871–13879.
[11] B. Herbig, P. Löbmann, J. Photochem. Photobiol. A: Chem. 163 (2004) 359–365.
[12] H. Yu, S.C. Lee, J. Yu, C.H. Ao, J. Mol. Catal. A: Chem. 246 (2005) 206–211.
[13] I. Zumeta, B. González, R. Espinosa, J.A. Ayllón, E. Vigil, Semicond. Sci. Technol. 19 (2004) L52–L55.
[14] (a) X.P. Wang, Y. Yu, X.F. Hu, L. Gao, Thin Solid Films 371 (2000) 148–152;
(b) Y. Gao, Y. Masuda, K. Koumoto, Langmuir 20 (2004) 3188–3194.
[15] D. Gutiérrez-Tauste, X. Domènech, M.A. Hernández-Fenollosa, J.A. Ayllón, J. Mater. Chem. 16 (2006) 2249–2255.
[16] (a) T.P. Niessen, M.R. De Guire, Solid State Ionics 151 (2002) 61–68;
(b) Y. Gao, K. Koumoto, Cryst. Growth Des. 5 (2005) 1983–2017.
[17] S.Y. Choi, M. Mamak, N. Coombs, N. Chopra, G.A. Ozin, Nano Lett. 4 (2004) 1231–1235.
[18] M. Biancardo, R. Argazzi, C.A. Bignozzi, Inorg. Chem. 44 (2005) 9619–9621.
[19] M. Grätzel, Nature 414 (2001) 338–344.
[20] T. Rajh, Z. Saponjic, J. Liu, N.M. Dimitrijevic, N.F. Scherer, M. Vega-Arroyo, P. Zapol, L.A. Curtiss, M.C. Thurnauer, Nano Lett. 4 (2004) 1017–1023.
[21] D. Gutiérrez-Tauste, I. Zumeta, E. Vigil, M.A. Hernández-Fenollosa, X. Domènech, J.A. Ayllón, J. Photochem. Photobiol. A: Chem. 175 (2005) 165–171.

[22] M. Nishizawa, S. Kuwabata, H. Yoneyama, J. Electrochem. Soc. 143 (1996) 3462–3465.
[23] H. Yanagi, T. Hishiki, T. Tobitani, A. Otomo, S. Mashiko, Chem. Phys. Lett. 292 (1998) 332–338.
[24] R. Shacham, D. Avnir, D. Mandler, J. Sol–Gel Sci. Technol. 31 (2004) 329–334.
[25] M.H. Bartl, S.W. Boettcher, E.L. Hu, G.D. Stucky, J. Am. Chem. Soc. 126 (2004) 10826–10827.
[26] L. Li, M. Mizuhata, S. Deki, Appl. Surf. Sci. 239 (2005) 292–301.
[27] L. Li, M. Mizuhata, A. Kajinami, S. Deki, Synth. Met. 146 (2004) 17–27.
[28] L. Feng, Y. Liu, J. Hu, Langmuir 20 (2004) 1786–1790.
[29] T. Oekermann, T. Yoshida, H. Minoura, K.G.U. Wijayantha, L.M. Peter, J. Phys. Chem. B 18 (2004) 8364–8370.
[30] T. Pauporté, F. Bedioui, D. Lincot, J. Mater. Chem. 15 (2005) 1552–1559.
[31] T. Mabuchi, S. Satoshi, T. Nakajima, J. Ino, K. Takemura, E. Shimizu, J. Photosci. 5 (1998) 105–109.
[32] T. Usui, S. Suzuki, M. Kojima, T. Nakajima, J. Ino, K. Takemura, Mol. Cryst. Liquid Cryst. Sci. Technol. 277 (1996) 215–226.
[33] H. Yao, N. Li, S. Xu, J.Z. Xu, J.J. Zhu, H.Y. Chen, Biosens. Bioelectron. 21 (2005) 372–377.
[34] D. Chatterjee, S. Dasgupta, N.N. Rao, Sol. Energy Mater. Sol. C 90 (2006) 1013–1020.
[35] S.K. Lee, A. Mills, A. Lepre, Chem. Commun. (2004) 1912–1913.
[36] S.K. Lee, M. Sheridan, A. Mills, Chem. Mater. 17 (2005) 2744–2751.
[37] K. Nakamoto, Infrared and Raman Spectra of Inorganic and Coordination Compounds. Part A: Theory and Applications in Inorganic Chemistry, 5th ed., Wiley-Interscience, New York, 1997.
[38] H. Park, W. Choi, J. Phys. Chem. B 108 (2004) 4086–4093.
[39] Y. Yan, M. Zhang, K. Gong, L. Su, Z. Guo, L. Mao, Chem. Mater. 17 (2005) 3457–3463.
[40] E. Brasell, J. Phys. Chem. 72 (1968) 2477–2483.
[41] Z. Zhao, E.R. Malinowski, J. Chemometr. 13 (1999) 83–94.
[42] F. Gessner, C.C. Schmitt, M.G. Neumann, Langmuir 10 (1994) 3749–3753.
[43] D. Heger, J. Jirkovsky, P. Klan, J. Phys. Chem. A 109 (2005) 6702–6709.
[44] A.K. Ghosh, P. Mukerjee, J. Am. Chem. Soc. 92 (1970) 6413–6415.
[45] S. Jockusch, N.J. Turro, D.A. Tomalia, Macromolecules 28 (1995) 7416–7418.
[46] D. Severino, H.C. Junqueira, M. Gugliotti, D.S. Gabrielli, M.S. Baptista, Photochem. Photobiol. 77 (2005) 459–468.
[47] A. Mills, J. Wang, J. Photochem. Photobiol. A: Chem. 127 (1999) 123–134.
[48] K. Patil, R. Pawar, P. Talap, Phys. Chem. Chem. Phys. 2 (2000) 4313–4317.
[49] S. Bodoardo, L. Borello, S. Fiorilli, E. Garrone, B. Onida, C. Otero-Areán, N. Penazzi, G. Turnes-Palomino, Micropor. Mesopor. Mater. 79 (2005) 275–281.